

Designing spin and orbital exchange Hamiltonians with ultrashort electric field transients

Martin Eckstein,¹ Johan H. Mentink,² and Philipp Werner³

¹Max Planck Institute for the structure and Dynamics of Matter 22761 Hamburg, Germany

²Radboud University Nijmegen, Institute of Molecules and Materials,
Heyendaalseweg 135, 6525 AJ Nijmegen, The Netherlands

³Department of Physics, University of Fribourg, 1700 Fribourg, Switzerland

We demonstrate how electric fields with arbitrary time profile can be used to control the time-dependent parameters of spin and orbital exchange Hamiltonians. Analytic expressions for the exchange constants are derived from a time-dependent Schrieffer-Wolff transformation, and the validity of the resulting effective Hamiltonian is verified for the case of a quarter-filled two-orbital Hubbard model, by comparing to the results of a full nonequilibrium dynamical mean-field theory simulation. The ability to manipulate Hamiltonians with arbitrary time-dependent fields, beyond the paradigm of Floquet engineering, opens the possibility to control intertwined spin and orbital order using laser or THz pulses which are tailored to minimize electronic excitations.

PACS numbers: 71.10.Fd, 72.10.Di, 05.70.Ln

Femtosecond laser pulses provide intriguing opportunities for manipulating and even switching between phases of complex materials on ultrafast time scales [1, 2]. Many successful scenarios to trigger ultrafast phase transitions rely on the excitation of non-equilibrium electron distributions, i.e. by photo doping or ultrafast heating [3–7]. As a result, the photo-induced dynamics proceeds by relaxation of photo-excited carriers that is irreversible on ultrafast time scales. Clearly, a highly appealing scenario beyond photo-excitation is to achieve full control of the quantum many-body dynamics even during the excitation pulse, which could enable a reversible manipulation of optically induced phase transitions.

In recent years, the problem of such ultrafast and reversible control of solids has been attacked by engineering light-dressed Hamiltonians with off-resonant time-periodic perturbations. The evolution of a system over one period of the external field is described by a so-called Floquet Hamiltonian H_F , which can be manipulated by the amplitude and frequency of the field. This can be used to control tunneling [8], change the topology of bands [9–12], and to manipulate many-body interactions such as spin-exchange [13–15] or superconducting pairing [16–19]. In this letter, we would like to extend on this in two directions: First, (i), we investigate the potential of designing light-induced interactions in the particularly interesting case of intertwined spin and orbital order, which is a hallmark of correlated materials [20]. Orbital interactions are often frustrated, which leads to rich phase diagrams, and nontrivial light-induced dynamics, including switching to hidden states [21–26]. Secondly, (ii), when trying to make use of light-induced interactions in solids, a fundamental limit is set by the energy absorption from the drive. Theoretically, H_F can be derived in the ideally off-resonant limit of high-frequencies [27–31], but in real solids absorption is usually low only in small frequency windows. As an alternative, strong few-cycle optical or THz pulses are available for the control of solids [32–36], so it is an interesting question whether light-dressed Hamiltonians can be generalized to transient pulses, down to the single-cycle limit, and how to optimize the pulse parameters. In this paper, we address these

questions by first generalizing the control of spin-exchange Hamiltonians to the case of electric field pulses of arbitrary shape, and apply this approach to the manipulation of Hamiltonians with coupled spin and orbital exchange interactions, i.e. the celebrated Kugel-Khomskii interactions [37].

A standard approach to derive low-energy Hamiltonians are perturbative unitary transformations, which remove the transition matrix elements between high-energy states (charge excitations) and low energy states, as in the derivation of the Heisenberg spin model from the Hubbard model [38]. One can generalize the approach by searching for a *time-dependent unitary transformation* to a rotating frame, in which the Hamiltonian does not mix the charge and spin sector *at any time*. In the rotating frame, the dynamics of the low-energy sector is governed by time-dependent exchange interactions that depend on time-dependent electric fields. To carry out this program, which was already done for an attractive Hubbard model [39] (and for the time-periodic case [15, 40]), we separate the Hilbert space into the low-energy and excited sector \mathcal{H}_0 and \mathcal{H}_1 , respectively, with projectors \mathcal{P}_0 and $\mathcal{P}_1 = 1 - \mathcal{P}_0$, and decompose each operator A into transitions $A_{ab} \equiv \mathcal{P}_a A \mathcal{P}_b$ between and within the sectors [41]. Furthermore, we assume that the Hamiltonian $H = V_{11} + \alpha T$ has an interaction V_{11} which acts in \mathcal{H}_1 , and the remainder T is controlled by a small parameter $\alpha \ll 1$. In strong-coupling perturbation theory, e.g., T is the hopping. For any time-dependent unitary transformation $e^{S(t)}$ (parametrized by the antihermitian matrix S), which transforms the wave function like $|\Psi_{rot}(t)\rangle = e^{S(t)}|\Psi(t)\rangle$, the Hamiltonian in the rotated frame is $H_{rot}(t) = e^{S(t)}[H - i\partial_t]e^{-S(t)}$. A Taylor ansatz $S = \alpha S_1 + \alpha^2 S_2 + \dots$ yields the series

$$H_{rot}(t) = V + \alpha \{T + [S_1, V] + i\dot{S}_1\} + \alpha^2 \{[S_2, V] + i\dot{S}_2 + [S_1, T] + \frac{1}{2}[S_1, i\dot{S}_1 + [S_1, V]]\} + \mathcal{O}(\alpha^3). \quad (1)$$

One can now truncate the expansion of S after a given order n , and choose S_n such that $H_{rot} = \sum_{m=0}^n \alpha^m H^{(m)} + \mathcal{O}(\alpha^{n+1})$ has no mixing terms for $m \leq n$, $H_{01}^{(m)} = H_{10}^{(m)} = 0$. At first order, we request that the first bracket in (1) should have no

mixing terms. The resulting differential equation for S_1 yields

$$S_{1,10}(t) = - \int d\bar{t} G_V^R(t, \bar{t}) T_{10}(\bar{t}), \quad (2)$$

where we introduced the Green's function $G_V^R(t, t') = -i e^{-i[V-i0^+](t-t')}\theta(t-t')$ (0^+ is a positive infinitesimal). When this expression is inserted into the next order, we have

$$H_{00}^{(2)} = -\frac{1}{2}(T_{01}S_{1,10} + h.c.). \quad (3)$$

Equations (2) and (3) constitute the general expression for any time-dependent low-energy model to second order, which will now be evaluated for the case of spin and orbital exchange interactions.

As a first illustration, we consider the one-band half-filled Hubbard model

$$H(t) = -t_0 \sum_{\langle ij \rangle \sigma} (e^{i\phi_{ij}(t)} c_{i\sigma}^\dagger c_{j\sigma} + h.c.) + \sum_i U n_{i\uparrow} n_{i\downarrow}. \quad (4)$$

Here $c_{i\sigma}$ denotes the annihilation operators of a fermion with spin σ at the lattice site i , U the on-site interaction; $t_0 e^{i\phi_{ij}(t)}$ is the hopping integral (restricted to nearest neighbour sites), with a time-dependent Peierls phase $\phi_{ij}(t) = \int_0^t d\bar{t} \vec{E}(\bar{t}) \cdot (\vec{r}_i - \vec{r}_j)$ that captures the effect of an electric field $\vec{E}(t)$. Taking V and T as the interaction and time-dependent hopping term, respectively, we can evaluate Eqs. (2) and (3) assuming $U \gg t_0$. At half-filling, the result is the standard spin-1/2 Heisenberg model $H_{00}^{(2)} = \sum_{\langle i,j \rangle} J_{\text{ex}}^{ij}(t) \vec{S}_i \cdot \vec{S}_j$, with time-dependent exchange interaction along a bond (i, j) ($U^+ = U + i0^+$),

$$J_{\text{ex}}^{ij}(t) = 4t_0^2 \text{Im} \int_{-\infty}^t d\bar{t} e^{iU^+(t-\bar{t})} \cos[\phi_{ij}(t) - \phi_{ij}(\bar{t})]. \quad (5)$$

The integral generalizes the energy denominator $1/U$ in the time-independent (zero field) exchange $J_{\text{ex,eq}} = 4t_0^2/U$.

In Fig. 1a we plot Eq. (5) for an oscillating field $E(t)$ with gaussian envelope. The time-dependent field generates a $J_{\text{ex}}(t)$ which has oscillatory and non-oscillatory components, but deviates on average from the equilibrium value $4t_0^2/U$. One easily verifies that Eq. (5) reproduces the limits of time-independent and time-periodic fields: A dc electric field with projection E_{ij} along the bond (i, j) , $\phi_{ij}(t) = -E_{ij}t$, gives $J_{\text{ex,dc}}(E_{ij}) = 2t_0^2/(U - E_{ij}) + 2t_0^2/(U + E_{ij})$. This dc modification of exchange has been derived from time-independent perturbation theory (taking into account an electrostatic potential), and was observed in cold atom experiments [42]. Furthermore, for a time-periodic field $E_{ij}(t) = A_{ij}\omega \cos(\omega t)$ ($\phi_{ij}(t) = A_{ij} \sin(\omega t)$), Eq. (5) yields, up to terms oscillating with frequency ω , the exchange interaction $J_{\text{ex,fl}}(A_{ij}, \omega) = \sum_n \frac{4t_0^2 \mathcal{J}_n(A_{ij})^2}{U - n\omega}$ known from Floquet theory [13] ($\mathcal{J}_n(x)$ is the Bessel function).

Using the general expression (5) it is interesting to check the range of validity of the Floquet expression in the experimentally relevant regime of few-cycle pulses. For this we compare the exact expression to the dc result $J_{\text{ex,dc}}(E(t))$,

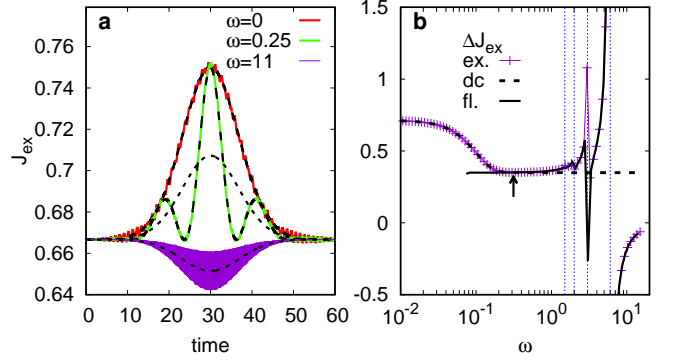


Figure 1. (a) Time-dependent exchange interaction [Eq. (5)] in the Hubbard model ($U = 6$ and $J = 1$), for an oscillating electric field $E(t) = E_0 \cos(\omega(t - t_c))e^{-(t-t_c)^2/t_c^2}$ with gaussian envelope of duration $t_c = 10$ and frequency ω . Dashed and dotted lines refer to the instantaneous dc and Floquet exchange $J_{\text{ex,dc}}(E(t))$ and $J_{\text{ex,fl}}(E_{\text{env}}(t)/\omega, \omega)$, respectively. (b) Modification of $J_{\text{ex}}(t) - J_{\text{ex}}(0)$, integrated over the duration of the pulse. The exact result (symbols) is compared to the instantaneous dc (dashed line) and Floquet (solid line) expressions. Vertical dotted lines indicate the resonances $n\omega = U$ of the Floquet exchange, the arrow indicates the single-cycle pulse frequency $\omega = \pi/t_c$.

evaluated using the instantaneous electric fields, as well as to the Floquet result $J_{\text{ex,fl}}(E_{\text{env}}(t)/\omega, \omega)$, evaluated at the instantaneous envelope of the field (see dashed and dotted lines in Fig. 1a). To quantify the difference between the expressions, we compare the integral $\Delta J_{\text{ex}} = \int dt (J_{\text{ex}}(t) - J_{\text{ex}}(0))$ in the three cases, see Fig. 1b. This quantity is related to a possible induced spin dynamics during the pulse. Remarkably, the Floquet expression works down to the limit of a single cycle pulse ($\omega \approx \pi/t_c$), except close to the resonances $n\omega = U$ (vertical lines). One can also see that there are various choices of the field amplitude and frequency with the same effect on J_{ex} , which leaves room for optimizing the pulse parameters in order to minimize the electronic excitations. This will be addressed below for the case of field-induced orbital dynamics.

As second illustration, we show how Eq. (5) is generalized to systems with intertwined spin and orbital exchange interactions. We consider $3d$ orbitals in a cubic crystal field, with inactive (filled or empty) t_{2g} states, and one electron in the two-fold degenerate e_g manifold. This situation is described by the two-orbital Hubbard model, with rotationally invariant interaction V and hopping T ,

$$\begin{aligned} V &= U \sum_{i,l} n_{i\uparrow} n_{i\downarrow} + \sum_{i,\sigma\sigma',l \neq l'} (U' - J_H \delta_{\sigma\sigma'}) n_{i\sigma} n_{i\sigma'} \\ &+ J_H \sum_{i,l \neq l'} (c_{i\uparrow}^\dagger c_{i\downarrow}^\dagger c_{i\downarrow} c_{i\uparrow} + c_{i\uparrow}^\dagger c_{i\downarrow}^\dagger c_{i\downarrow} c_{i\uparrow}) \\ T(t) &= - \sum_{\langle ij \rangle \sigma, l l'} (t_{ll'} e^{i\phi_{ij}(t)} c_{i\sigma}^\dagger c_{j\sigma} + h.c.). \end{aligned} \quad (6)$$

Here $l = 0, 1$ labels the $d_{3z^2-r^2}$ and $d_{x^2-y^2}$ orbital, respectively, J_H is the Hunds-coupling, and $U' = U - 2J_H$. As the Coulomb interaction U projects out doubly occu-

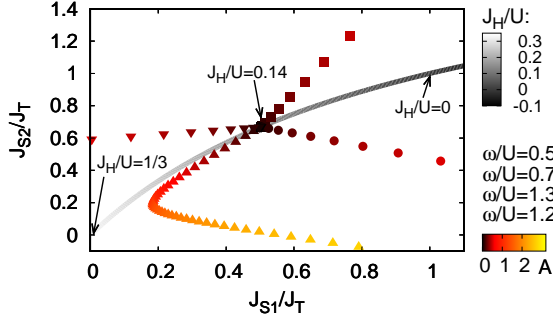


Figure 2. Ratio of the (period-averaged) exchange constants $J_{1,2,3}(A, \omega)$ in Eq. (10) for a time periodic field $E(t) = A\omega \cos(\omega t)$ along a given bond, for $J_H/U = 0.14$. The symbols indicate different frequencies, and the color map shows the amplitude. The line shows the accessible parameter space in equilibrium, for different values of J_H as indicated by the grey-scale.

pied sites, the model reduces to a low-energy Hamiltonian for spins \vec{S}^i and orbital pseudo-spins $\vec{Z}^i \equiv (Z_1^i, Z_2^i, Z_3^i)$, $Z_a^i = \frac{1}{2} \sum_{\sigma\ell} c_{i\ell\sigma}^\dagger \sigma_{\ell\sigma}^a c_{i\ell\sigma}$ (σ^a for $a = 1, 2, 3$ are Pauli matrices), which is the Kugel-Khomskii model.

We follow Ref. [43] to parametrize this model [44]. Since the hopping is rotationally invariant in spin, the exchange Hamiltonian on each bond (i, j) can be factorized as

$$h^{ij} = \left(\frac{3}{4} + \vec{S}^i \vec{S}^j\right) K_T^{ij} + \left(\frac{1}{4} - \vec{S}^i \vec{S}^j\right) K_S^{ij}, \quad (8)$$

where the terms in brackets are projectors on the spin triplet and singlet, respectively, and $K_{S,T}$ is the orbital part of the Hamiltonian. Due to the geometry of the orbitals, the latter depends on the direction of the bond. In a cubic crystal, hopping t_0 along the z direction is possible only between the $d_{3z^2-r^2}$ orbitals, so that $K_{S,T}^z$ takes a simple form

$$\begin{aligned} K_S^{ij,z} &= J_{S1}^z (Z_3^i Z_3^j - \frac{1}{4}) - (J_1^z + J_{S2}^z) (\frac{1}{2} + Z_3^i) (\frac{1}{2} + Z_3^j), \\ K_T^{ij,z} &= J_T^z (Z_3^i Z_3^j - \frac{1}{4}). \end{aligned} \quad (9)$$

Here $J_s^z = 2t_0^2/\varepsilon_s$ correspond to the possible energies $\varepsilon_{S1} = U + J_H$, $\varepsilon_{S2} = U - J_H$, $\varepsilon_T = U - 3J_H$ of a doublet, which appear as virtual states in second-order perturbation theory. Along the x and y bonds, \vec{Z} spinors have to be replaced by the spinors \vec{X} and \vec{Y} corresponding to $(d_{3x^2-r^2}, d_{y^2-z^2})$ and $(d_{3y^2-r^2}, d_{z^2-x^2})$, which relate to \vec{Z} by a 120° rotation around the orbital pseudo-spin-2 axis, $X_3 = -\frac{1}{2}(-\sqrt{3}Z_1 + Z_3)$, $Y_3 = -\frac{1}{2}(\sqrt{3}Z_1 + Z_3)$. The orbital part of (9) is thus highly anisotropic and favors mutual alignment in different orbitals along different directions, which is an intrinsically frustrated so-called Kompass model [46].

In the time-dependent case [Eq. (3)], it is important to note that the time-dependence of the hopping enters as a global (orbital independent) Peierls factor in Eq. (7), and V is time independent. The geometrical structure of the Hamiltonian is therefore unchanged, while the exchange constants J_s^α along the $\alpha = x, y, z$ bonds are obtained by replacing the energy

denominators $1/\varepsilon_s$ by a time-integral as in Eq. (5),

$$J_s^\alpha(t) = 2t_0^2 \text{Im} \int_{-\infty}^t d\bar{t} e^{i\varepsilon_s^+(t-\bar{t})} \cos[\phi_\alpha(t) - \phi_\alpha(\bar{t})]. \quad (10)$$

This time-dependent manipulation of the exchange in the Kugel-Khomskii model suggests various possibilities to act on spin and orbital order. For example, a time-dependent field allows to tune separately the ratios of the three exchange constants, as illustrated in Fig. 2 for a time-periodic field. While in equilibrium the ratio J_{S1}/J_T and J_{S2}/J_T is only a function of J_H/U , in nonequilibrium, one can both access parameter regimes which correspond to a different ratio J_H/U , and those regimes which are inaccessible in equilibrium.

Below we verify Eq. (10) by discussing light-induced orbital dynamics. We will focus on a simple situation where the spin direction is entirely polarized, such that only the triplet term in Eq. (9) contributes, which is the antiferro-orbital 120° Kompass model. It is instructive to first look at the classical mean-field dynamics of the orbital model. Assuming anti-ferro-orbital order with $\langle \vec{Z}^i(t) \rangle \equiv \vec{\tau}_\pm(t)$ for site i on either of the two sublattices (labelled \pm), we obtain mean-field equations of motion $\frac{d}{dt} \vec{\tau}_\pm(t) = \vec{B}_\pm(t) \times \vec{\tau}_\pm(t)$, with an orbital pseudo-magnetic field that has contributions from each of the two neighbors along the $\alpha = x, y, z$ bonds, $B_{\pm,\alpha}(t) = 2 \sum_{\alpha,b} J_T^\alpha(t) \eta_{ab}^\alpha \tau_{\mp,b}(t)$; the geometry of the exchange along the different bonds is captured by the tensor

$$\eta^{x(y)} = \frac{1}{4} \begin{pmatrix} 3 & 0 & \pm\sqrt{3} \\ 0 & 0 & 0 \\ \pm\sqrt{3} & 0 & 1 \end{pmatrix}, \eta^z = \begin{pmatrix} 0 & 0 & 0 \\ 0 & 0 & 0 \\ 0 & 0 & 1 \end{pmatrix}. \quad (11)$$

One can see that in equilibrium, with $J_T^x = J_T^y = J_T^z \equiv J_{\text{ex}}$, any configuration in the orbital (Z_1, Z_3) plane corresponds to an equilibrium solution, with $\vec{B}_\pm = 3J_{\text{ex}} \vec{\tau}_\mp$. An external field, polarized along one axis, *independently* modifies the exchange along the three bond directions, and thus induces a precessional dynamics [47].

To confirm the prediction from the strong-coupling analysis (10), we now solve the nonequilibrium dynamics of the spin-polarized two-band Hubbard model under the influence of an electric field, using nonequilibrium DMFT [49]. This technique, which maps the lattice model onto a set of coupled single-impurity models, has been described elsewhere, and we defer the details of the implementation to the appendix. The model is solved on the cubic lattice with a simplified closed form self-consistency, using a hybridization expansion impurity solver [50]. We consider the insulating regime at $U - 3J_H = 6$ and bandwidth $W = 4$ at initial (inverse) temperature $\beta = 30$, which corresponds to antiferro-orbital order along the z -direction, with $|\langle \vec{Z}_3 \rangle| \approx 0.32$.

Figure 3a shows the time-evolution of the ordered orbital moment on one sublattice during and after a gaussian field pulse, with polarization along the x -direction. For smaller fields ($E_0 \leq 5$), the evolution of the transverse Z_1 and Z_2 components of the orbital order follows the mean-field solution of the spin model, obtained with the time-dependent $J_T(t)$ from Eq. (10) (dashed lines).

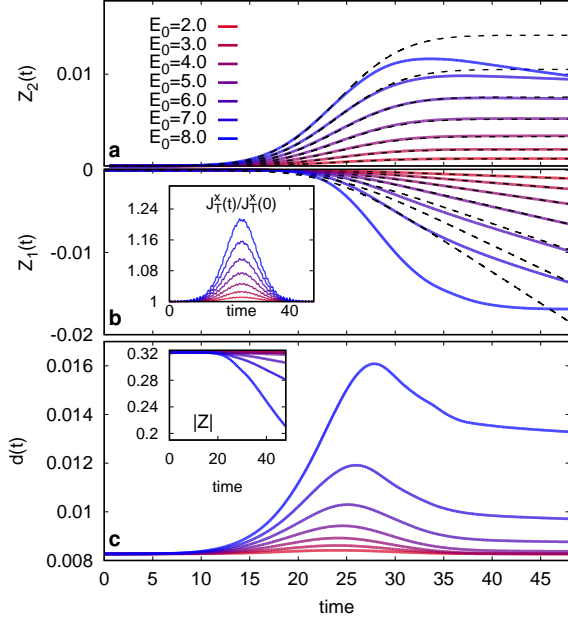


Figure 3. Orbital dynamics induced by an electric field $E_x(t) = E_0 e^{-(t-t_c)^2/t_c^2}$ in a cubic environment ($U - 3J_H = 6$, $J = 1$, $\beta = 30$). The initial state is anti-ferro orbital order in the orbital pseudo-spin z direction. (a) and (b) Z_2 and Z_1 for various field amplitudes. The dashed lines correspond to the solution of the mean-field dynamics, with time-dependent exchange interaction given by (10) (see inset in panel b; $J_T^y(t) = J_T^z(t) = J_T^x(0)$ remain unchanged by the field). (c) Change of the double occupancy, and the total ordered orbital moment $|\vec{Z}|$ for the same pulses.

The orbital pseudo-magnetic field $B_{\pm}(t)$ always lies in the (Z_1, Z_3) plane, but due to the bond-dependent exchange coupling (inset in Fig. 3b) it is rotated from the original Z_3 direction, such that the precessional motion generates a component Z_2 , which corresponds to a complex superposition of the $d_{3z^2-r^2}$ and $d_{x^2-y^2}$ orbital. For larger fields, the DMFT results decrease during the pulse compared to the spin model. This can be understood as the strong fields induce charge excitations, which have been projected out in the unitary perturbation theory. This is confirmed in Fig. 3c, where we show that the double occupancy $d(t)$ is increased after the pulse (the increase during the pulse corresponds to virtual fluctuations). For a high density of excitations, the orbital ordered moment $|\vec{Z}|$ starts to decrease after the pulse (see inset), in analogy to the melting of antiferromagnetic spin order by photo-doping [51].

Finally, we use the same DMFT setup to find the parameters that realize a desired effect on the ordered state at the least amount of electronic excitation. Figure 4 shows a color map of the absorption, measured in terms of the increase Δd of the double occupancy, for pulses within a range of frequencies and field amplitudes, keeping the duration $t_c = 8$ of the pulse fixed. The vertical axis is the accumulated precession of the

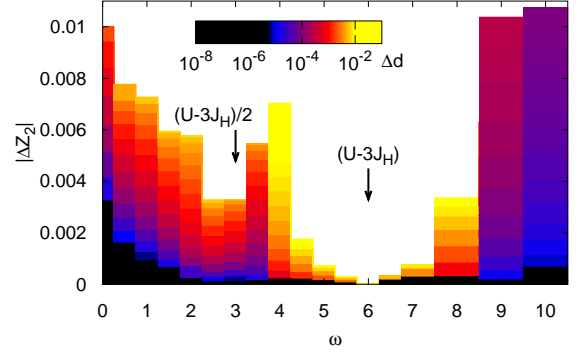


Figure 4. For the few-cycle $E(t) = E_0 \cos(\omega(t - t_c))e^{-(t-t_c)^2/t_c^2}$ with given duration $t_c = 8$, the color map shows the excitation density (increase Δd of the double occupancy after the pulse), as a function of the frequency, and the achieved orbital precession (change $|\Delta Z_2|$ during the pulse).

component Z_2 , which first increases with the field, but cannot exceed a certain maximum as excitations set in at larger amplitudes. One finds that close to the resonance $U - 3J_H = \omega$, and to some extent $U - 3J_H = 2\omega$, almost no precession can be obtained, as absorption processes strongly compete with the off-resonant dynamics described by the effective exchange Hamiltonian. We observe that to induce a certain effect in the most reversible way, it is best to go to the quasi-dc regime, corresponding to THz excitation in the Mott insulator. Alternatively, one can go to the high-frequency regime, but in real solids there are typically charge excitations to other electronic bands that are not captured in the present simulations.

In conclusion, we have demonstrated the manipulation of spin and orbital exchange Hamiltonians with electric fields of arbitrary time-profile. A time-dependent Schrieffer-Wolff transformation provides an important guiding principle for the evaluation of the effective exchange interactions, as we quantitatively verified by solving the full electronic model which includes the absorption due to field-induced tunnelling or (multi)photon absorption. In particular, in order to control exchange interactions in the most reversible way, our analysis strongly favors low frequency, quasi dc, electric fields corresponding to THz excitation of the Mott insulator.

These findings suggest many possibilities for future studies. Firstly, orbital ordering is often coupled to Jahn-Teller distortions of the lattice. In this case, the field induced exchange interactions provide one part of the force on the ordering, and it will be interesting to study the combined effect. Moreover, the actual order in the orbital models is not rotationally invariant like in spacial mean field simulations, but entropically stabilized in certain directions due to non-local fluctuations [52]. Another interesting and open problem is therefore to study the dynamics of a (classical or quantum) model with time-dependent J_{ex} , taking into account these entropic forces. Finally, our results suggests that it is very interesting to investigate the THz manipulation of exchange Hamiltonians for reversible control of magnetic order at ultralow energy load.

ME acknowledges support by the DFG within the Sonderforschungsbereich 925 (project B4). PW acknowledges support from FP7 ERC Starting Grant No. 278023. JM was supported by the Nederlandse Organisatie voor Wetenschappelijk Onderzoek (NWO) through a VENI grant.

APPENDIX

In this appendix we give the detailed equations for the implementation of nonequilibrium DMFT for the two-band Hubbard model with e_g orbitals. We start from the Hamiltonian Eq. (6) and (7) of the main text, which describes electrons on two orbitals of e_g symmetry at each site, and adopt the parametrization of the orbitals as described in Ref. [46], where orbital 1 and 2 correspond to orbitals $d_{x^2-y^2}$ and $d_{3z^2-r^2}$, respectively. We introduce the orbital spinor (omitting site and spin indices for simplicity)

$$\hat{\psi} = \begin{pmatrix} c_1 \\ c_2 \end{pmatrix} \equiv \begin{pmatrix} c_{x^2-y^2} \\ c_{3z^2-r^2} \end{pmatrix}. \quad (12)$$

The Wannier orbitals transform among each other like the atomic e_g orbitals, which have wave functions $\phi_{x^2-y^2}(\vec{r}) = \phi(r)(x^2 - y^2)$ and $\phi_{3z^2-r^2}(\vec{r}) = \phi(r)(3z^2 - r^2)/\sqrt{3}$, with some radial part $\phi(r)$. By forming linear combinations of $d_{x^2-y^2}$ and $d_{3z^2-r^2}$, one arrives at the other basis states $d_{y^2-z^2}$, $d_{z^2-x^2}$, $d_{3x^2-r^2}$, and $d_{3y^2-r^2}$. These linear combinations can be conveniently represented as rotations in orbital-pseudospin space, generated by ($\sigma_{1,2,3}$ denote the Pauli matrices)

$$\hat{R}(\theta) = e^{i\hat{\sigma}_2\theta/2} = \begin{pmatrix} \cos(\theta/2) & \sin(\theta/2) \\ -\sin(\theta/2) & \cos(\theta/2) \end{pmatrix}. \quad (13)$$

Rotations by $\theta = 4\pi/3$ give,

$$\hat{R}\left(\frac{4}{3}\pi\right)\hat{\psi} = \begin{pmatrix} -\frac{1}{2}c_{x^2-y^2} + \frac{\sqrt{3}}{2}c_{3z^2-r^2} \\ -\frac{\sqrt{3}}{2}c_{x^2-y^2} - \frac{1}{2}c_{3z^2-r^2} \end{pmatrix} = \begin{pmatrix} c_{z^2-x^2} \\ c_{3y^2-r^2} \end{pmatrix}, \quad (14)$$

where the last equality can be checked by evaluating the operators on the one-particle states, e.g., $\langle 0 | -\frac{1}{2}c_{x^2-y^2} + \frac{\sqrt{3}}{2}c_{3z^2-r^2} | \vec{r} \rangle = -\frac{1}{2}\phi_{x^2-y^2}(\vec{r})^* + \frac{\sqrt{3}}{2}\phi_{3z^2-r^2}(\vec{r})^* = \phi(r)^*[-\frac{1}{2}(x^2 - y^2) + \frac{\sqrt{3}}{2}(2z^2 - x^2 - y^2)/\sqrt{3}] = \phi_{z^2-x^2}(\vec{r})^* = \langle 0 | c_{z^2-x^2} | \vec{r} \rangle$. In summary, successive application of $\hat{R}(4\pi/3)$ corresponds to a permutation of the orbitals $xyz \rightarrow zxy \rightarrow yzx \rightarrow xyz$ [46].

With the orbital spinor, the hopping is written as

$$T = - \sum_{j\sigma} \sum_{a=x,y,z} \left(e^{i\phi_a(t)} \hat{\psi}_{j+\hat{e}_a,\sigma}^\dagger \hat{v}_a \hat{\psi}_{j,\sigma} + h.c. \right), \quad (15)$$

where \hat{e}_a denotes the unit vector along a bond direction a , $\phi_a(t) = \phi_{j+\hat{e}_a,j}$ is the Peierls phase along the bond ($j+\hat{e}_a, j$), and \hat{v}_a is a 2×2 matrix. As stated in the main text, we focus

on a cubic environment, in which the only nonvanishing matrix element for hopping along the z axis is between $d_{3z^2-r^2}$ orbitals,

$$\hat{v}_z = \begin{pmatrix} 0 & 0 \\ 0 & t_0 \end{pmatrix}. \quad (16)$$

To obtain the hopping along the x -bond, we first rotate the lattice around the y axis, which maps $x \rightarrow z$ and $z \rightarrow -x$, so that the hopping along the x -bond is then written as

$$\begin{pmatrix} c_{z^2-y^2}^\dagger & c_{3x^2-r^2}^\dagger \\ 0 & t_0 \end{pmatrix} \begin{pmatrix} 0 & 0 \\ 0 & t_0 \end{pmatrix} \begin{pmatrix} c_{z^2-y^2} \\ c_{3x^2-r^2} \end{pmatrix}. \quad (17)$$

Analogous to Eq. (14) we get

$$\hat{R}\left(-\frac{4}{3}\pi\right) \begin{pmatrix} c_{x^2-y^2} \\ c_{3z^2-r^2} \end{pmatrix} = -\hat{\sigma}_3 \begin{pmatrix} c_{z^2-y^2} \\ c_{3x^2-r^2} \end{pmatrix}, \quad (18)$$

so that Eq. (17) (and the corresponding equation for the y -bond) becomes $\hat{\psi}^\dagger \hat{v}_{x/y} \hat{\psi}$, with (the sign σ_3 cancels)

$$\hat{v}_x = \hat{R}\left(\frac{4}{3}\pi\right) \hat{v}_z \hat{R}\left(-\frac{4}{3}\pi\right) = \frac{t_0}{4} \begin{pmatrix} 3 & -\sqrt{3} \\ -\sqrt{3} & 1 \end{pmatrix}, \quad (19)$$

$$\hat{v}_y = \hat{R}\left(-\frac{4}{3}\pi\right) \hat{v}_z \hat{R}\left(\frac{4}{3}\pi\right) = \frac{t_0}{4} \begin{pmatrix} 3 & \sqrt{3} \\ \sqrt{3} & 1 \end{pmatrix}. \quad (20)$$

In DMFT, we compute the 2×2 contour-ordered Green's function

$$\hat{G}(t, t') = -i \langle T_C \hat{\psi}_\sigma(t) \hat{\psi}_\sigma^\dagger(t') \rangle \quad (21)$$

$$\equiv \begin{pmatrix} G_{11}(t, t') & G_{12}(t, t') \\ G_{21}(t, t') & G_{22}(t, t') \end{pmatrix}. \quad (22)$$

(For an introduction into the Keldysh formalism for contour-ordered Green's functions and to nonequilibrium dynamical mean-field theory, see Ref. [49].) The DMFT impurity action is given by ($H_{loc} = V$ is the local interaction)

$$\mathcal{S} = -i \int_C dt H_{loc}(t) - i \sum_\sigma \int_C dt dt' \hat{\psi}_\sigma^\dagger(t) \hat{\Delta}(t, t') \hat{\psi}_\sigma(t'), \quad (23)$$

with a self-consistently determined hybridization matrix $\hat{\Delta}$, and \hat{G} is determined by $\hat{G}(t, t') = -i \text{tr}[T_C e^{\mathcal{S}} \hat{\psi}_\sigma(t) \hat{\psi}_\sigma^\dagger(t')] / \mathcal{Z}$.

For the DMFT simulation, we focus on a bipartite Bethe lattice in the limit of infinite coordination number $6Z \rightarrow \infty$, in which each site has Z bonds attached with rescaled hopping $-e^{i\phi_a(t)} \hat{v}_a / \sqrt{6Z}$ for each of the 6 combinations $\eta = \pm$, $a = x, y, z$. This can be envisioned as the simple limit of an infinitely coordinated lattice with a local cubic environment. As in the single band case, results can be expected to be qualitatively the same as for a three-dimensional cubic lattice with the bandwidth $4t_0$. Denoting by $\hat{G}_{A,B}$ the Green's function on the two sublattices A, B of the bipartite lattice, the DMFT self-consistency is given by

$$\hat{\Delta}_A(t, t') = \frac{1}{6} \sum_{a=x,y,z} \left(e^{i\phi_a(t)} \hat{v}_a \hat{G}_B(t, t') \hat{v}_a e^{-i\phi_a(t')} + e^{-i\phi_a(t)} \hat{v}_a \hat{G}_B(t, t') \hat{v}_a e^{i\phi_a(t')} \right) \quad (24)$$

(the derivation uses the cavity approach, analogous to the single-band case [53]).

The strong-coupling limit of the e_g Hubbard model is characterized by an entangled spin and orbital dynamics. Here we focus on the case where the spin is fully polarized. We can omit the spin index, and the local Hamiltonian reduces to

$$H_{loc} = \sum_j [(U - 3J_H)n_{j,1}n_{j,2} - \mu(n_{j,1} + n_{j,2})]. \quad (25)$$

The model thus becomes equivalent to a spin-less single-band model with orbital-dependent hopping, and we use the standard strong-coupling expansion [50] to solve the impurity model in the strongly interacting Mott regime. We allow for Néel-type anti-ferro-orbital sublattice symmetry breaking, and look for solutions in which the Green's function on site B is obtained from site A by a π rotation in orbital space,

$$\hat{G}_B(t, t') = \hat{R}(\pi)\hat{G}_A(t, t')\hat{R}(-\pi), \quad (26)$$

which closes the DMFT equations.

It is instructive to verify the symmetries for the DMFT equations (23), (24), (25), (26): One can show that in equilibrium (i.e., for $\phi_a = 0$) the solution is rotationally invariant around the σ_z axis in orbital pseudospin, i.e., if \hat{G} is a solution, $\hat{G}(\theta) \equiv \hat{R}(\theta)\hat{G}\hat{R}(-\theta)$ is a solution as well for all θ . To show this we rotate the spinors, $\hat{\psi}(\theta) \equiv R(\theta)\hat{\psi}$, so that $\hat{G}(\theta)(t, t') = -i\text{tr}[T_c e^{\mathcal{S}} \hat{\psi}(\theta)(t)\hat{\psi}(\theta)^\dagger(t')]/Z$. The interaction is rotationally invariant, $H_{loc}[\hat{\psi}^\dagger, \hat{\psi}] = H_{loc}[\hat{\psi}^\dagger(\theta), \hat{\psi}(\theta)]$, and the hybridization can be written as $-i \int_{\mathcal{C}} dt dt' \hat{\psi}^\dagger(\theta)(t)\hat{R}(\theta)\hat{\Delta}(t, t')\hat{R}(-\theta)\hat{\psi}(\theta)(t')$. We can see that $\hat{G}(\theta)(t, t')$ is a solution of the DMFT equations if the rotated hybridization function $\hat{R}(\theta)\hat{\Delta}_A(t, t')\hat{R}(-\theta)$ satisfies the self-consistency (24) with the rotated Green's function, i.e.,

$$\begin{aligned} \hat{R}(\theta) \left[\sum_{a=x,y,z} v_a \hat{G}_B(t, t') \hat{v}_a \right] \hat{R}(-\theta) \\ \stackrel{!}{=} \sum_{a=x,y,z} \hat{v}_a \hat{R}(\theta) \hat{G}_B(t, t') \hat{R}(-\theta) \hat{v}_a, \end{aligned} \quad (27)$$

which can be written as

$$I(\theta) \equiv \sum_{a=x,y,z} \hat{v}_a(\theta) \hat{G}_B(t, t') \hat{v}_a(\theta) \stackrel{!}{=} I(0), \quad (28)$$

with $\hat{v}_z(\theta) = \hat{R}(-\theta)\hat{v}_z\hat{R}(\theta)$. Using Eq. (19) and (20), we get

$$I(\theta) = \sum_{n=-2,0,2} \hat{v}_z(\theta + \frac{2n\pi}{3}) \hat{G}_B(t, t') \hat{v}_z(\theta + \frac{2n\pi}{3}). \quad (29)$$

Explicit evaluation gives

$$\begin{aligned} \hat{v}_z(\phi) \hat{G} \hat{v}_z(\phi) &= G_{11} \begin{pmatrix} s^4 & -s^3c \\ -s^3c & s^2c^2 \end{pmatrix} + G_{22} \begin{pmatrix} s^2c^2 & -sc^3 \\ -sc^3 & c^4 \end{pmatrix} \\ &+ (G_{12} + G_{21}) \begin{pmatrix} -s^3c & -s^2c^2 \\ -s^2c^2 & -sc^3 \end{pmatrix}, \end{aligned} \quad (30)$$

with $s \equiv \sin(\phi/2)$ and $c \equiv \cos(\phi/2)$. After summation in Eq. (29) we get,

$$I(\theta) = \frac{1}{8} \begin{pmatrix} 9G_{11} + 3G_{22} & -3(G_{12} + G_{21}) \\ -3(G_{12} + G_{21}) & 3G_{11} + 9G_{22} \end{pmatrix}, \quad (31)$$

independent of θ . This implies that the DMFT solutions will be rotationally invariant in equilibrium, which is a consequence of the spacial mean-field character of the equations: In the real lattice, the mean-field pseudospin solution is rotationally invariant, and the rotational invariance is broken to the lattice point group only by the order-by-disorder mechanism, which takes into account fluctuations of the order parameter around the long range order (spin waves), which are not correctly captured in DMFT [46].

-
- [1] C. Giannetti, M. Capone, D. Fausti, M. Fabrizio and F. Parmigiani, and D. Mihailovic, "Ultrafast optical spectroscopy of strongly correlated materials and high-temperature superconductors: a non-equilibrium approach", *Adv. in Phys.* **65**, 58 (2016).
 - [2] A. Kirilyuk and A. V. Kimel and T. Rasing, "Ultrafast optical manipulation of magnetic order", *Rev. Mod. Phys.* **82**, 2731 (2010).
 - [3] T. A. Ostler et al., "Ultrafast heating as a sufficient stimulus for magnetization reversal in a ferrimagnet", *Nat. Commun.* **3**, 666 (2012).
 - [4] L. Stojchevska, I. Vaskivskiy, T. Mertelj, P. Kusar, D. Svetin, S. Brazovskii, and D. Mihailovic, "Ultrafast Switching to a Stable Hidden Quantum State in an Electronic Crystal", *Science* **344**, 177 (2014).
 - [5] D. Wegkamp *et al.*, "Instantaneous Band Gap Collapse in Photoexcited Monoclinic VO₂ due to Photocarrier Doping", *Phys. Rev. Lett.* **113**, 216401 (2014).
 - [6] S. Mor *et al.*, "Ultrafast electronic band gap control in an excitonic insulator", arXiv:1608.05586.
 - [7] A. Stupakiewicz, K. Szerenos, D. Afanasiev, A. Kirilyuk and A. V. Kimel, "Ultrafast nonthermal photo-magnetic recording in a transparent medium", *Nature* **542**, 71 (2017).
 - [8] D. H. Dunlap and V. M. Kenkre, "Dynamic localization of a charged particle moving under the influence of an electric field", *Phys. Rev. B* **34**, 3625 (1986).
 - [9] T. Oka and H. Aoki, "Photovoltaic Hall effect in graphene", *Phys. Rev. B* **79**, 081406 (2009).
 - [10] T. Kitagawa, T. Oka, A. Brataas, L. Fu, E. Demler, "Transport properties of nonequilibrium systems under the application of light: Photoinduced quantum Hall insulators without Landau levels", *Phys. Rev. B* **84**, 235108 (2011).
 - [11] Y. H. Wang, H. Steinberg, P. Jarillo-Herrero, and N. Gedik, "Observation of Floquet-Bloch States on the Surface of a Topological Insulator", *Science* **342**, 453 (2013).
 - [12] G. Jotzu, M. Messer, R. Desbuquois, M. Lebrat, Th. Uehlinger, D. Greif, and T. Esslinger, "Experimental realization of the topological Haldane model with ultracold fermions", *Nature* **515**, 237 (2014).
 - [13] J. H. Mentink, K. Balzer, and M. Eckstein, "Ultrafast and reversible control of the exchange interaction in Mott insulators", *Nature Comm.* **6**, 6708 (2015).
 - [14] R. V. Mikhaylovskiy *et al.*, "Ultrafast optical modification of

- exchange interactions in iron oxides”, *Nature Comm.* **6**, 8190 (2015).
- [15] M. Bukov, M. Kolodrubetz, and A. Polkovnikov, “Schrieffer-Wolff Transformation for Periodically Driven Systems: Strongly Correlated Systems with Artificial Gauge Fields”, *Phys. Rev. Lett.* **116**, 125301 (2016).
- [16] M. Knap, M. Babadi, G. Refael, I. Martin, E. Demler, “Dynamical Cooper pairing in nonequilibrium electron-phonon systems”, *Phys. Rev. B* **94**, 214504 (2016).
- [17] A. Komnik and M. Thorwart, “BCS theory of driven superconductivity”, *Euro. Phys. Jour. B* **89**, 244 (2016).
- [18] J. Coulthard, S. R. Clark, S. Al-Assam, A. Cavalleri, D. Jaksch, “Enhancement of super-exchange pairing in the periodically-driven Hubbard model”, arXiv:1608.03964.
- [19] Y. Murakami, N. Tsuji, M. Eckstein, and P. Werner, “Nonequilibrium steady states and transient dynamics of superconductors under phonon driving”, arXiv:1702.02942.
- [20] Y. Tokura and N. Nagaosa, “Orbital Physics in Transition-Metal Oxides”, *Science* **288**, 462 (2000).
- [21] M. Rini, R. Tobey, N. Dean, J. Itatani, Y. Tomioka, Y. Tokura, R. W. Schoenlein, and A. Cavalleri, “Control of the electronic phase of a manganite by mode-selective vibrational excitation”, *Nature* **449**, 72 (2007).
- [22] D. Polli, M. Rini, S. Wall, R. W. Schoenlein, Y. Tomioka, Y. Tokura, G. Cerullo, and A. Cavalleri, “Coherent orbital waves in the photo-induced insulator-metal dynamics of a magnetoresistive manganite”, *Nature Materials* **6**, 643 - 647 (2007).
- [23] S. Wall, D. Prabhakaran, A. T. Boothroyd, and A. Cavalleri, “Ultrafast Coupling between Light, Coherent Lattice Vibrations, and the Magnetic Structure of Semicovalent LaMnO_3 ”, *Phys. Rev. Lett.* **103**, 097402 (2009).
- [24] M. Först *et al.*, “Driving magnetic order in a manganite by ultrafast lattice excitation”, *Phys. Rev. B* **84**, 241104 (2011).
- [25] H. Ichikawa *et al.*, “Transient photoinduced ‘hidden’ phase in a manganite”, *Nat. Mater* **10**, 101 (2011).
- [26] P. Beaud *et al.*, “A time-dependent order parameter for ultrafast photoinduced phase transitions”, *Nat. Mater.* **923**, 13 (2014).
- [27] N. Goldman and J. Dalibard, “Periodically Driven Quantum Systems: Effective Hamiltonians and Engineered Gauge Fields”, *Phys. Rev. X* **4**, 031027 (2014).
- [28] M. Bukov, L. D’Alessio, and A. Polkovnikov, “Universal high-frequency behavior of periodically driven systems: from dynamical stabilization to Floquet engineering”, *Adv. in Physics* **64**, 139 (2015).
- [29] A. Eckardt and E. Anisimovas, “High-frequency approximation for periodically driven quantum systems from a Floquet-space perspective”, *New Jour. of Phys.* **17**, 093039 (2015).
- [30] A. P. Itin and M. I. Katsnelson “Effective Hamiltonians for Rapidly Driven Many-Body Lattice Systems: Induced Exchange Interactions and Density-Dependent Hoppings”, *Phys. Rev. Lett.* **115**, 075301 (2015).
- [31] T. Mikami, S. Kitamura, K. Yasuda, N. Tsuji, T. Oka, and H. Aoki, Hideo, “Brillouin-Wigner theory for high-frequency expansion in periodically driven systems: Application to Floquet topological insulators”, *Phys. Rev. B* **93**, 144307 (2016).
- [32] T. Kampfrath *et al.*, “Coherent terahertz control of antiferromagnetic spin waves”, *Nat. Photon.* **5**, 31 (2011).
- [33] O. Schubert *et al.*, “Sub-cycle control of terahertz high-harmonic generation by dynamical Bloch oscillations”, *Nat. Photon.* **8**, 119 (2014).
- [34] T. Ishikawa *et al.*, “Optical freezing of charge motion in an organic conductor”, *Nature Comm.* **5**, 5528 (2014).
- [35] S. Baierl *et al.*, “Terahertz-Driven Nonlinear Spin Response of Antiferromagnetic Nickel Oxide”, *Phys. Rev. Lett.* **117**, 197201 (2016).
- [36] S. Baierl, M. Hohenleutner, T. Kampfrath, A. K. Zvezdin, A. V. Kimel, R. Huber, and R. V. Mikhaylovskiy, “Nonlinear spin control by terahertz-driven anisotropy fields”, *Nat. Photon.* **10**, 715 (2016).
- [37] K. I. Kugel and D. I. Khomskii, “The Jahn-Teller effect and magnetism: transition metal compounds”, *Sov. Phys. Uspekhi* **25**, 231(1982).
- [38] A. B. Harris and R. V. Lange, “Single-Particle Excitations in Narrow Energy Bands”, *Phys. Rev.* **157**, 295 (1967).
- [39] S. Kitamura and H. Aoki, “ η -pairing superfluid in periodically-driven fermionic Hubbard model with strong attraction”, *Phys. Rev. B* **94**, 174503 (2016).
- [40] E. Canovi, M. Kollar, and M. Eckstein, “Stroboscopic prethermalization in weakly interacting periodically driven systems”, *Phys. Rev. E* **93**, 012130 (2016).
- [41] K. A. Chao, J. Spalek and A. M. Oleś, “Kinetic exchange interaction in a narrow S-band”, *J. Phys. C* **10**, L271 (1977).
- [42] L.-M. Duan, E. Demler, and M. Lukin, “Controlling Spin Exchange Interactions of Ultracold Atoms in Optical Lattices”, *Phys. Rev. Lett.* **91**, 090402 (2003).
- [43] A. M. Oleś, L. F. Feiner, and J. Zaanen, “Quantum melting of magnetic long-range order near orbital degeneracy: Classical phases and Gaussian fluctuations”, *Phys. Rev. B* **61**, 6257 (2000).
- [44] Other, slightly different parameterizations based on a non-rotationally invariant interaction Hamiltonian have been considered in the literature [45].
- [45] S. Ishihara, J. Inoue, and S. Maekawa, “Electronic structure and effective Hamiltonian in perovskite Mn oxides”, *Physica C* **263**, 130 (1996).
- [46] Z. Nussinov and J. van den Brink, “Compass models: Theory and physical motivations”, *Rev. Mod. Phys.* **87**, 1 (2015).
- [47] Note that this is fundamentally different from photo-induced spin dynamics [48], where a change of exchange induces a spin precession only in the non-collinear ordered phase.
- [48] J. H. Mentink and M. Eckstein, “Ultrafast Quenching of the Exchange Interaction in a Mott Insulator”, *Phys. Rev. Lett.* **113**, 057201 (2014).
- [49] H. Aoki, N. Tsuji, M. Eckstein, M. Kollar, T. Oka, and Ph. Werner, “Nonequilibrium dynamical mean-field theory and its applications”, *Rev. Mod. Phys.* **86**, 779 (2014).
- [50] M. Eckstein and Ph. Werner, “Nonequilibrium dynamical mean-field calculations based on the noncrossing approximation and its generalizations”, *Phys. Rev. B* **82**, 115115 (2010).
- [51] Ph. Werner, N. Tsuji, and M. Eckstein, “Nonthermal symmetry-broken states in the strongly interacting Hubbard model”, *Phys. Rev. B* **86**, 205101 (2012).
- [52] J. van den Brink, P. Horsch, F. Mack, and A. M. Oleś “Orbital dynamics in ferromagnetic transition-metal oxides”, *Phys. Rev. B* **59**, 6795 (1999).
- [53] A. Georges, G. Kotliar, W. Krauth, and M. J. Rozenberg, “Dynamical mean-field theory of strongly correlated fermion systems and the limit of infinite dimensions”, *Rev. Mod. Phys.* **68**, 13 (1996).